CONF-961018--2 ANL/CMT/CP--87845

ALLOY WASTE FORMS FOR METAL FISSION PRODUCTS AND ACTINIDES ISOLATED BY SPENT NUCLEAR FUEL TREATMENT*

S. M. McDeavitt, D. P. Abraham, D. D. Keiser, Jr., and J. Y. Park

Argonne National Laboratory
Chemical Technology Division
9700 South Cass Avenue
Argonne, Illinois 60439

ABSTRACT

Waste form alloys are being developed at Argonne National Laboratory for the disposal of remnant metallic wastes from an electrometallurgical process developed to treat spent nuclear fuel. This metal waste form consists of the fuel cladding (stainless steel or Zircaloy), noble metal fission products (e.g., Ru, Pd, Mo and Tc), and other metallic wastes. The main constituents of the metal waste stream are the cladding hulls (85 to 90 wt%); using the hulls as the dominant alloying component minimizes the overall waste volume as compared to vitrification or metal encapsulation. Two nominal compositions for the waste form are being developed: (1) stainless steel-15 wt% zirconium for stainless steel-clad fuels and (2) zirconium-8 wt% stainless steel for Zircaloy-clad fuels. The noble metal fission products are the primary source of radiation in the metal waste form. However, inclusion of actinides in the metal waste form is being investigated as an option for interim or ultimate storage. Simulated waste form alloys were prepared and analyzed to determine the baseline alloy microstructures and the microstructural distribution of noble metals and actinides. Corrosion tests of the metal waste form alloys indicate that they are highly resistant to corrosion.

*Work supported by the U.S. Department of Energy, Nuclear Energy Research and Development Program, under Contract No. W-31-109-Eng. 38.

I. INTRODUCTION

Waste form alloys have been developed at Argonne National Laboratory for the immobilization of metallic materials left behind following the electrometallurgical treatment of spent nuclear fuel.[1-4] These alloys contain stainless steel and zirconium matrix metals and will be used to immobilize fission products and, possibly, actinide metals. The term "waste form" refers to radioactive materials and any encapsulating or stabilizing matrix that will be placed into a "waste package" for disposal. The radioactive materials may be stabilized for disposal by encapsulation, chemical transformation, and/or inclusion in a stable matrix material.

Vitrification in borosilicate glass has been widely selected as a primary stabilization method for high-level wastes.[5] However, several issues make vitrification an undesirable option for the metallic waste stream considered here. First, noble metal fission products (NMFPs) are strong crystal formers in vitrified waste forms, and crystal formation decreases the mechanical integrity of glass.[6] Since NMFPs are the primary radioactive constituent of the metal waste form, this problem cannot be avoided. Second, vitrification of the metallic waste stream would result in very significant mass and volume increases since the high-density metals would be converted into low-density oxides and combined with additional glass-forming material. For example, converting just the stainless steel and zirconium metals to oxide precursors for vitrification would result in a ~150% mass increase and ~200% volume increase, and that is before the addition of a base glass. Minimizing the waste form volume is critical because the unit volume cost for repository disposal is expected to be quite high. In addition to these fundamental issues, some practical process-related issues make a metal waste form desirable. For example, the electrometallurgical process is very compact and may be contained in a single inert-environment cell, which includes a waste form melting furnace. Opting for vitrification would require a large vitrification facility adjacent to the inert cell or transportation of the waste to a separate vitrification facility at an independent location. The electrometallurgical process eliminates the need for these two options.

The electrometallurgical treatment process will be undergoing a full-scale demonstration in the Fuel Conditioning Facility (FCF)[7] in conjunction with the shutdown and dismantling of the Experimental Breeder Reactor-II (EBR-II) at Argonne National Laboratory-West, Idaho. The principal step in this process is the electrorefining of uranium metal in a molten salt electrolyte.[8-9] Three distinct material streams emanate from the electrorefiner: (1) refined metallic uranium, (2) fission products and actinides extracted from the electrolyte salt that are processed into a ceramic waste form, and (3) metallic wastes that are consolidated into the metal waste form. The metal waste form comprises the spent fuel cladding, the NMFPs (e.g., Ru, Rh, Pd, Zr, and Tc) that do not dissolve in the electrolyte salt, and, in some cases, zirconium metal from alloy nuclear fuels. These metallic wastes are not generated in the electrorefiner; they are present with the spent fuel before treatment. The spent fuel cladding hulls and NMFPs are inert in the electrorefiner environment and, therefore, remain in the charge basket as the uranium, other actinides, and active fission products are electrochemically dissolved or transported.

Two types of fuel were used in EBR-II: driver fuel and blanket fuel.[10] The driver fuel is a U-10 wt% Zr alloy[a] with Type 316 and D9 stainless steel cladding, and the blanket fuel is uranium metal with Type 304 stainless steel cladding. The cladding materials plus the NMFP and Zr from the driver fuel will be melted together into a uniform, corrosion-resistant waste form. Approximately 0.5 to 4 wt% NMFP will be present in this metal waste form,

[a] All compositions are in wt% unless indicated otherwise.

depending on the fuel burnup. The alloying process will be carried out in a high-temperature, controlled-atmosphere melting furnace.[11] Although EBR-II fuel will be treated first, other spent fuels with stainless steel and Zircaloy claddings are being evaluated for future treatment.

In all cases, the cladding hulls represent over 85% of the metal waste stream. By using the hulls as the major alloying component, the total waste form volume is minimized. This approach gave rise to the parallel development of two compositions for the metal waste form: (1) stainless steel-15 wt% zirconium (SS-15Zr) for stainless steel-clad fuel and (2) Zircaloy-8 wt% stainless steel (Zr-8SS) for Zircaloy-clad fuel. The development effort on the metal waste form includes the ongoing evaluation of the physical metallurgy, corrosion performance, thermophysical properties, and process variables important to waste form generation and qualification. Metal waste forms containing actinide metals[4] are also of interest as a backup option to the present plan of incorporating the actinides extracted form the spent fuel into a ceramic waste form. This paper reports on the microstructural characterization of simulated SS-Zr waste forms of various compositions and results from preliminary corrosion tests of the SS-Zr alloys.

II. METAL WASTE FORM ALLOYS

The nominal alloy compositions SS-15Zr and Zr-8SS were selected on the basis of initial characterization and corrosion data. In addition, such parameters as alloying temperature and minimal nonwaste additions were also considered. The SS-15Zr composition is near a eutectic having a melt temperature of ~1330°C. The Zr-8SS composition is not near a eutectic, but its liquidus temperature is ~1500°C. Therefore, both alloys may be produced at temperatures near 1600°C. A large-scale tilt-pour casting furnace (3-kg capacity) was designed, built, and connected to an inert atmosphere glovebox for use in developing the waste form alloying procedures. This furnace is being used to generate large ingots and to test processing parameters.

Small-scale (~20 g) stainless steel-zirconium alloys were generated that had a range of zirconium compositions to simulate the SS-15Zr and Zr-8SS waste forms and other SS-Zr alloy compositions.[2] The alloys were prepared from stainless steel (Types HT9, 304, or 316), zirconium, and selected noble metals (i.e., Ru, Pd, Mo, and Ag). These materials were melted at 1600°C in yttria (Y_2O_3) crucibles under an argon atmosphere for 1 to 2 h and solidified by cooling slowly. The microstructural evolution and phase development of SS-Zr alloys with various Zr contents were studied by using scanning electron microscopy (SEM), energy dispersive X-ray analysis (EDX), and X-ray diffraction.[2] More recently, neutron diffraction has been used to characterize phases that have only a minor presence in the waste form alloys.

Stainless steel-rich alloys containing 5 to 40 wt% Zr exhibit varying proportions of an iron solid solution and a Laves-type intermetallic (AB_2 crystal structure) that we have designated $Zr(Fe,Cr,Ni)_{2+x}$.[2] The microstructure of the nominal waste form for stainless steel-clad fuel, SS-15Zr, is presented in Figure 1. As a first approximation, the SS-15Zr alloy contains a two-phase structure, where the dark phase is a ferritic Fe (α-Fe) solid solution, and the bright contrast phase is the intermetallic compound $Zr(Fe,Cr,Ni)_{2+x}$. The compositions of the various SS-15Zr alloy phases are given in Table I.

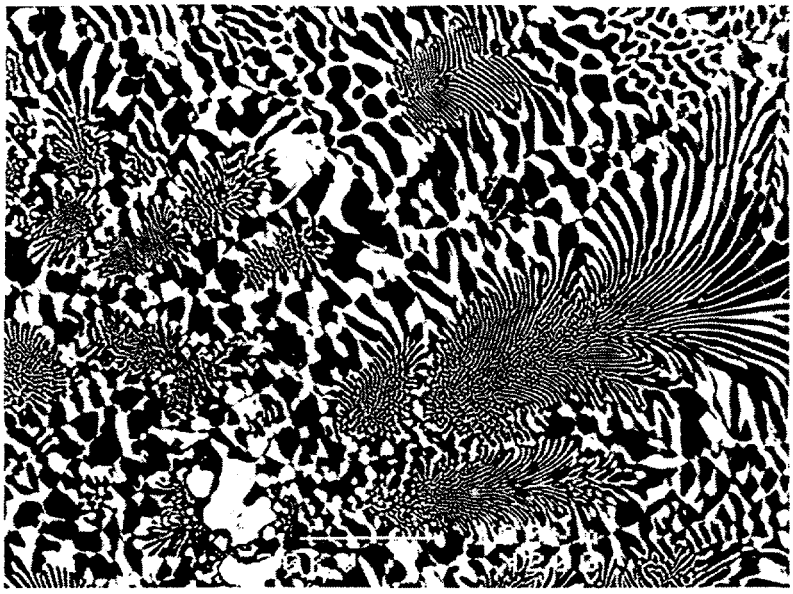

Figure 1. Backscattered Electron Image (200x) of SS-15Zr Eutectic Structure. The dark phase is an iron solid solution, and the bright phase is the $Zr(Fe,Cr,Ni)_{2+x}$ intermetallic.

Table I. Composition of Observed Phases in SS-15Zr and Zr-8SS Alloys*

	Phase	Crystal Structure	Fe	Zr	Cr	Ni
SS-15Zr	α-Fe	BCC	69	0	24	4
	γ-Fe	FCC	70	0	20	8
	$Zr(Fe,Cr,Ni)_{2+x}$	AB_2 Laves phase	54	24	8	11
	Zr_6Fe_{23}-Type	Th_6Mn_{23}-Type	57	19	10	9
Zr-8SS	α-Zr	HCP	3	94	1.5	0.5
	$Zr(Fe,Cr)_2$	AB_2 Laves phase	42	34	21	0
	$Zr_2(Fe,Ni)$	$CuAl_2$-Type	28	66	0	6

*Listed compositions are in atom % (±3%).

Below ~15 wt% Zr, the iron solid solution is found to be a mixture of α-Fe and austenitic Fe (γ-Fe), both of which contain Cr and Ni levels corresponding to those of ferritic and austenitic stainless steels.[2] A minor volume fraction of the γ-Fe phase is observed in SS-15Zr alloys generated with Type 316 stainless steel, whereas only the α-Fe phase is present when Type 304 stainless steel is used. This minor difference in structure is the result of a higher nickel content in Type 316 stainless steel vs. Type 304 stainless steel. The $Zr(Fe,Cr,Ni)_{2+x}$ intermetallic is a strong sink for Ni, an austenite stabilizer, but it saturates at low Zr concentrations, leaving excess Ni to stabilize the γ-Fe phase. The relative proportion of $Zr(Fe,Cr,Ni)_{2+x}$ increases with increasing zirconium concentration until ~40 wt% Zr, when the alloy is ~100% intermetallic and brittle.

In addition, a minor quantity of a different intermetallic phase was identified by neutron diffraction and then observed using SEM (Figure 2). This phase was determined to be Zr_6Fe_{23}, a stable Fe-Zr intermetallic phase.[12] A significant quantity of this phase is observed in slowly cooled alloys and after long-term annealing experiments. The $Zr(Fe,Cr,Ni)_{2+x}$ Laves phase is apparently metastable, consistent with literature predictions,[12] and it slowly transforms into the Zr_6Fe_{23}-type phase. Much of the performance-related data generated to date has been for as-cast alloys with the $Zr(Fe,Cr,Ni)_{2+x}$ as the dominant intermetallic in the microstructure. It has been determined, however, that a minor presence of the Zr_6Fe_{23}-type phase is likely to be present in all samples. A detailed investigation is being carried out to determine what effect, if any, this intermetallic will have on the performance of the metal waste form.

Zirconium-rich alloys (>40 wt% Zr) contain multi-phase mixtures of various brittle intermetallic phases up to ~84 wt% Zr (16 wt% SS).[2] As the Zr content increases from 84 to 100 wt%, a zirconium solid-solution phase (α-Zr) is observed in increasing quantity, along with decreasing quantities of the intermetallic phases. Figure 3 shows the microstructure of Zr-8SS, the nominal waste form alloy for Zircaloy-clad fuel. The Zr-8SS alloy possesses a multi-phase microstructure dominated by the primary α-Zr solid solution surrounded by a complex eutectic structure containing the α-Zr phase and intermetallic compounds; these intermetallics have been qualitatively identified to be $Zr_2(Fe,Ni)$ and $Zr(Fe,Cr)_2$, as shown in Table I.

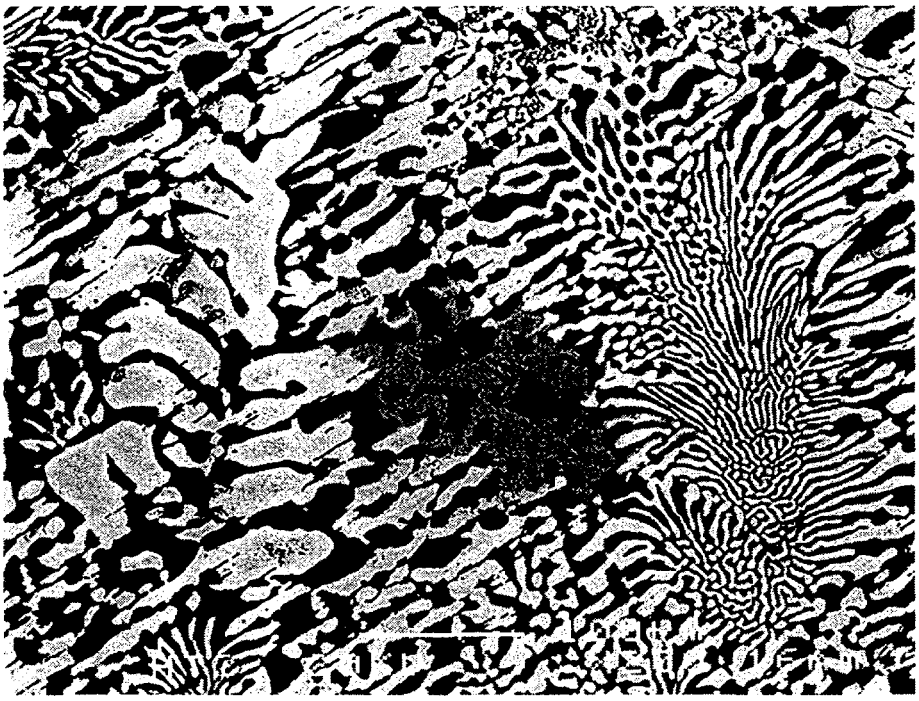

Figure 2. Backscattered Electron Image (200x) of Intermetallic Phase in SS-15Zr Alloy. The Zr_6Fe_{23}-type intermetallic phase (dark gray) forms upon transformation of the $Zr(Fe,Cr,Ni)_{2+x}$ Laves phase (light gray).

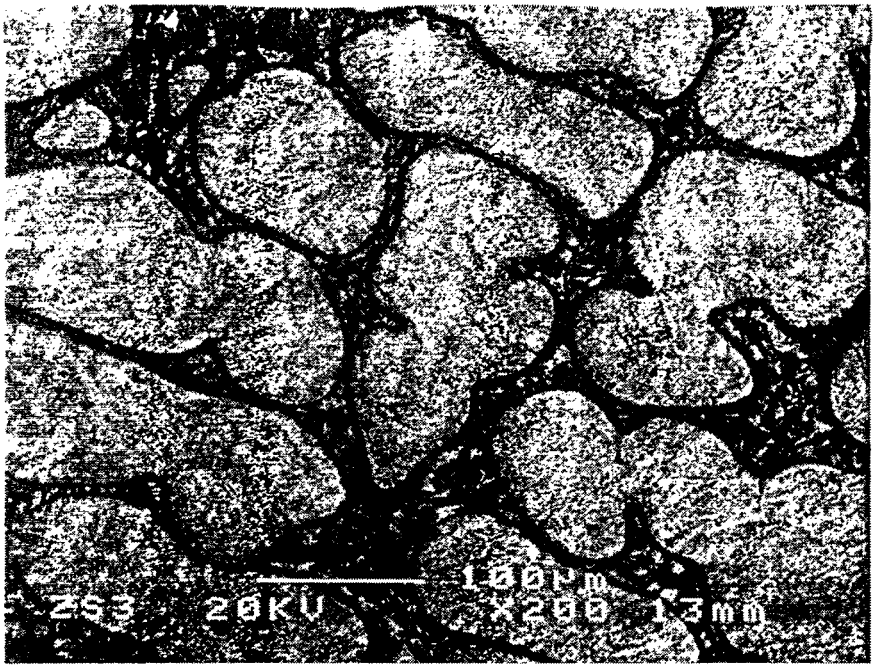

Figure 3. Backscattered Electron Image (200x) of Zr-8SS Structure. The major phase is a zirconium solid solution, and the darker phases are intermetallics.

III. NOBLE METAL FISSION PRODUCTS

The fission product composition in spent nuclear fuel is dependent upon the fuel's accumulated burnup. That is, as nuclear fission occurs, the fuel isotopes (e.g., U-235) split into a wide variety of lighter isotopes. The entire fission product inventory includes gases and chemically active isotopes that are not included in the metal waste stream. Noble metal fission products represent ~35% of the total fission product inventory. The actual quantity and composition of NMFPs present in a given metal waste stream are dependent on starting fuel composition, neutron energy spectrum, and the duration of irradiation.

The nuclear fuel modeling code, ORIGEN, was used to calculate the fission product inventory of EBR-II fuel[b] in its current state and at future times by simulating changes due to radioactive decay. The NMFP content in the driver fuel is expected to be as high as 2 to 4 wt%, whereas the NMFP content in the blanket is expected to be below 0.5 wt%. Each NMFP element is present as several isotopes, and the intense initial radioactivity comes from isotopes present in very minor concentrations. The metal waste form composition is, therefore, not significantly altered as the isotopes with high activity and short lifetime decay away. For example, ORIGEN predicts ~6.6 kg of Ru in EBR-II fuel with an initial activity of ~88,000 Ci, but the activity comes exclusively from an estimated 0.3 g of Ru-106 and Ru-103, which have half-lives of 372.6 d and 39.2 d, respectively.

The intense initial radioactivity decays rapidly as transmutation occurs. Figure 4 shows the time-dependent change in specific activity for an average EBR-II metal waste form. The radiation level drops precipitously over the first 100 years and settles into a long-term rate of decay dominated by long-lived NMFP isotopes, primarily Tc-99. The activity for the

[b] Calculation by R. N. Hill, Reactor Analysis Division, Argonne National Laboratory.

metal waste form is relatively benign when compared to spent light water reactor (LWR) fuel and other radioactive waste forms that may be permanently disposed of in a geologic repository. Similar ORIGEN calculations[b] indicate that the long-term specific activity of typical LWR spent fuel is on the order of 1 Ci/g, even after 10^6 years; all of this activity is attributed to the long-lived actinides that will remain in untreated spent fuel. The activity for the EBR-II metal waste form will be only ~0.05 Ci/g at its peak, and it decays rapidly to ~3 x 10^{-5} Ci/g in the first 100 y. This value is only two orders of magnitude higher than the specific activity of natural uranium oxide.

The noble metals Ru, Re, Pd, Mo, and Ag were added experimentally to SS-15Zr and Zr-8SS alloy samples to simulate the presence of NMFPs. The total noble metal content ranged from 1 to 5 wt% (a typical addition to SS-15Zr was 2 Ru-1.5 Pd-0.5 Ag). Examination of alloy microstructures revealed no discrete noble metal phases. No differences were seen between noble metal-containing microstructures and the baseline microstructures Figs. 1 and 3. For SS-15Zr alloys, the noble metals were dissolved and distributed between the intermetallic and the iron solid solution. Some elements (i.e., Ru, Pd, and Ag) showed a ~2:1 preference for the intermetallic phase, while others (i.e., Re) showed a similar preference for the iron solution. The noble metal distribution has not yet been quantified for the Zr-8SS alloy, but a similar absence of noble metal precipitation was seen. These observations indicate that the SS-Zr waste form alloys are indeed viable as NMFP disposition alloys.

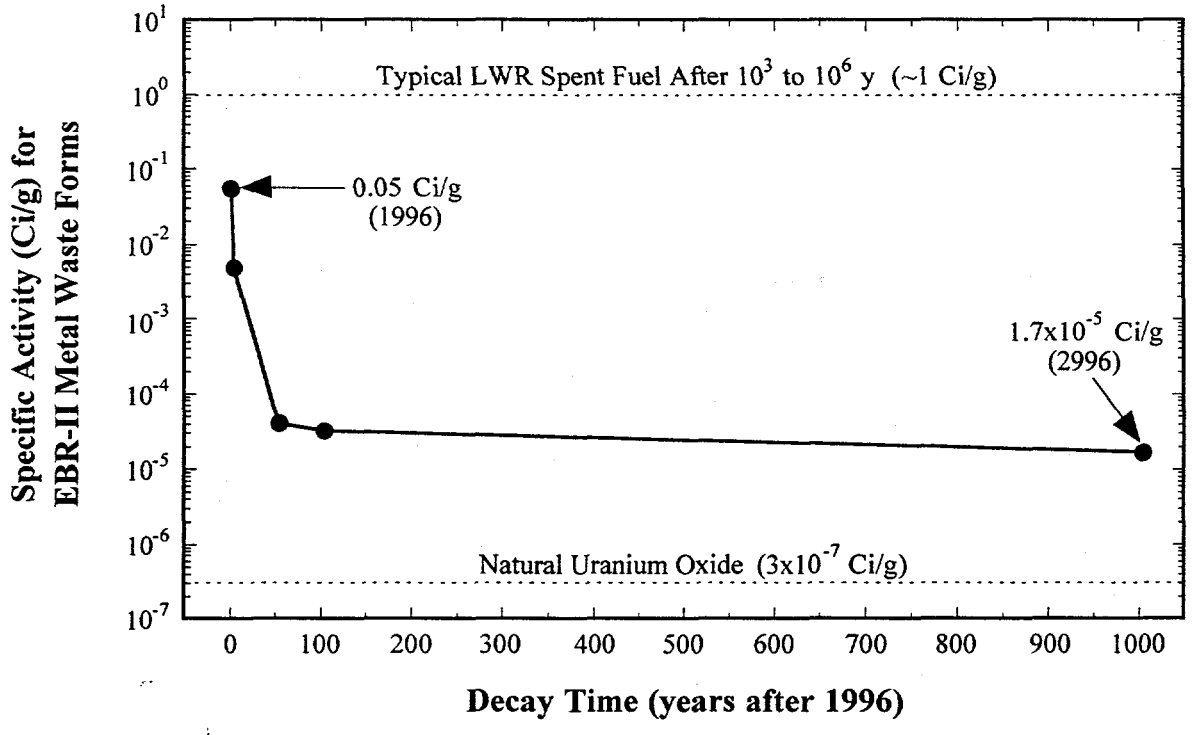

Figure 4. Calculated Specific Activity of EBR-II Metal Waste Form vs. Time

IV. ACTINIDE-BEARING WASTE FORMS

Small-scale samples of simulated waste form alloys (~30 g) containing uranium, plutonium, and neptunium were prepared in yttria crucibles by melting at 1600°C for 2 h under a flowing argon atmosphere, then cooling slowly to room temperature. The samples included SS-15Zr alloys with actinide compositions of 0.5U-0.5Pu, 2U-2Pu, 6Pu, 10Pu, 6Pu-2Np, and 2Np. Also prepared were Zr-8SS alloys with 4, 7, and 10 wt% Pu. The SS-15Zr alloys were generated using Type 316SS, and the Zr-8SS alloys were generated using Type 304SS. The range of actinide concentrations used in this study was selected to provide insight into the actinide interactions with the existing phases. If actinides are placed into the metal waste form in actual practice, instead of in a ceramic waste form, the actinide concentration will be between 1 and 10 wt%.

Figure 5 presents a representative microstructure for the actinide-bearing SS-15Zr alloys. The microstructure is similar to the baseline SS-15Zr microstructure shown in Figure 1, except for the presence of a high-contrast phase that is moderately rich in actinides. There is 2 at. % Pu in the $Zr(Fe,Cr,Ni)_{2+x}$ intermetallic but no actinides are detectable in the iron solid solution. The high-contrast phase in Figure 5 is an intermetallic that is apparently miscible with the $Zr(Fe,Cr,Ni)_{2+x}$ phase; its composition is 33 at. % Fe-33 at. % Ni-20 at. % actinide (U, Pu, and/or Np) plus small amounts of Zr, Cr, and other minor components. This phase was observed in all of the actinide-bearing SS-15Zr alloys, irrespective of the actinide or group of actinides; increasing the actinide content resulted in a higher volume fraction of this phase.

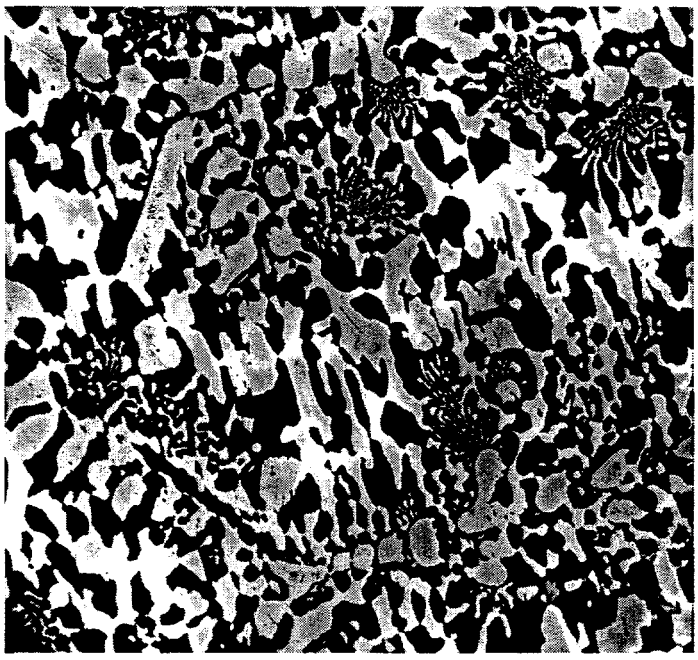

Figure 5. Backscattered Electron Image of SS-15Zr Alloy Containing 2 wt% U and 2 wt% Pu. The bright contrast phases are rich in U and Pu.

In SS-15Zr samples where multiple actinides were added, up to 20 at. % actinide was observed in the high-contrast phase. Furthermore, changes in the zirconium content of the $Zr(Fe,Cr,Ni)_{2+x}$ phase were observed in Np-bearing alloys. The Zr content was as low as 13 at. % in the sample with 2 at. % Np. For actinide-bearing alloys without Np, the Zr content in the $Zr(Fe,Cr,Ni)_{2+x}$ phase was ~22 at. %, similar to the 24 at. % reported for the baseline alloy in Table I. The Fe solid solution did not exhibit concentration differences.

Figure 6 presents a representative microstructure for the Zr-8SS-xPu alloys. Again, the microstructure resembles the corresponding baseline alloy (Figure 3). The Pu was observed in solution in the α-Zr metal matrix, but it was also found in higher concentrations at the α-phase boundaries (i.e., the bright spike-like features in Figure 6). The formation of these Pu-rich features may be explained as follows: (1) the high-temperature zirconium metal phase, β-Zr, is completely miscible with the high-temperature plutonium metal phase, ε-Pu, but the low-temperature zirconium metal phase, α-Zr, has limited solubility for plutonium (<13 at. %); (2) the β-Zr metal forms first upon cooling, with up to 100% of the plutonium in solution; (3) β-Zr transforms to α-Zr at ~863°C; and (4) the excess Pu that exceeds α-Zr solubility becomes concentrated at newly formed α-Zr phase boundaries. Increasing the amount of Pu added to the alloy from 4 to 10 wt% resulted in higher amounts of Pu both in the α-Zr matrix phase (from 1.5 to 5 at. % Pu) and at the α-phase boundaries (up to 12 at. % Pu).

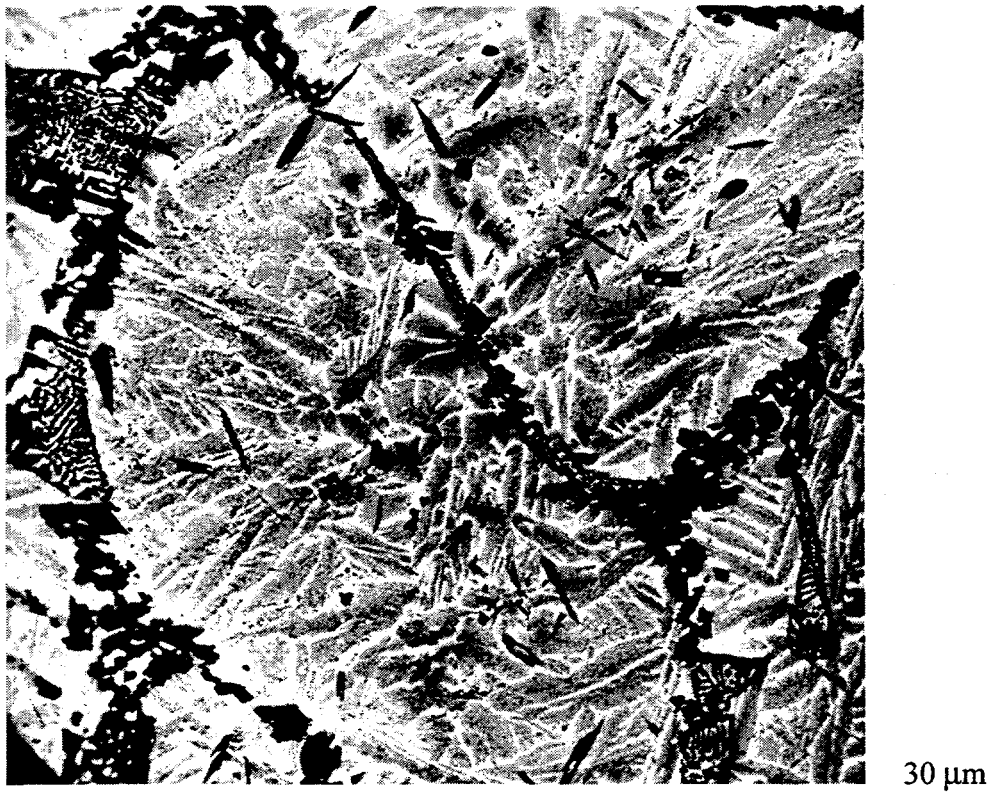

Figure 6. Backscattered Electron Image of Zr-8SS Alloy Containing 10 wt% Pu (300x). The bright-contrast features are α-Zr phase boundaries with ~12 at. % Pu.

Neither actinide-bearing alloy exhibits pure actinide phases. Since the actinides are entrained in complex, but stable, matrix phases, the SS-Zr alloy waste forms have potential application as actinide disposal alloys. Performance testing must be carried out to verify this hypothesis; however, since Pu has only a minor effect on the alloy microstructure, the performance of the baseline alloys (discussed earlier) may be used to infer the performance of the actinide-bearing alloys, as a first approximation. Equipment is being assembled to begin a testing program to evaluate the performance of actinide-bearing alloys.

V. WASTE FORM EVALUATION

Small-scale samples with various zirconium contents were machined and polished into disks and tested using general immersion and electrochemical corrosion methods. Corrosion testing was typically carried out using simulated J-13 well water, which is representative of the groundwater at the Yucca Mountain site in Nevada that has been proposed for a high-level nuclear waste repository. The ionic concentration of J-13 well water is (in mg/L): 11.5 Ca, 1.76 Mg, 45.0 Na, 5.3 K, 0.06 Li, 0.04 Fe, 0.001 Mn, 0.03 Al, 30.0 Si, 2.1 F^-, 6.4 Cl^-, 18.1 SO_4^{2-}, 10.1 NO_3^-, 143.0 HCO_3^-, and 5.7 dissolved oxygen.

General immersion corrosion tests were carried out using a test procedure based on the MCC-1 Static Leach Test, which was developed for glass-based waste forms. Disk specimens, 15.9-mm diameter and 3-mm thick, were polished to a 600 grit finish, immersed in the J-13 solution in a sealed Teflon vessel, and placed in an oven at 90°C. Test specimens made from SS-15Zr and Zr-8SS alloys and other off-nominal Zr compositions were tested. However, the test solution was benign to the stainless steel-zirconium alloys, and corrosion rates were not measurable. In fact, most of the surfaces of the immersion specimens remained shiny after exposure durations up to 10,000 h (381 d). Table II presents the mass loss data measured for several SS-15Zr alloys and a Zr-8SS alloy after exposure to J-13 well water for 10,000 h. The measured mass differences are so small that they are statistically zero (the resolution of the balance used to make the measurements is ±0.0001 g). This is a very positive result, but it does not provide a quantitative means to evaluate the corrosion resistance or the leach resistance of the alloys.

Table II. General Corrosion Results after 10,000 h in J-13 Well Water

Alloy (in wt%)	Mass (g) Initial	After 10,000 h	Mass Change (g)
Zr-8SS	4.0683	4.0681	- 0.0002
SS-15Zr	4.2362	4.2361	-0.0001
SS-15Zr	3.1385	3.1386	+0.0001
SS-15Zr	3.5995	3.5994	-0.0001
SS-15Zr-2Ru-1.5Pd-0.5Ag	3.9197	3.9198	+0.0001
SS-15Zr-2Ru-1.5Pd-0.5Ag	3.8389	3.8388	-0.0001

Another test method employed was to measure the corrosion rate by the electrochemical linear polarization method. This method can measure very low corrosion rates in a short duration. The electrochemical cell current is measured and mathematically converted

into a uniform corrosion rate; localized corrosion may affect this measurement, but we have not observed any evidence of this effect. Measurements were made at pH = 2, 4, 7, and 10 to cover a range of potential repository conditions; pH = 2 represents an extreme acidic condition that may not occur in the repository environment, but it provides an aggressive test to compare the relative performance of these low-corrosion-rate metals.

The electrochemical corrosion rates are shown in Table III for the waste form alloys, commercial zirconium and stainless steel, and selected candidate canister materials. The waste form corrosion rates at pH = 7 for the waste form alloys are comparable or slightly lower than the measured rates for Types 316 and 304 stainless steel and zirconium metal. Noble metal additions do not significantly affect the corrosion rates of the waste form alloys. Also, their corrosion rates are similar to the rate for Incoloy 825, lower than the rate for pure copper, and two orders of magnitude lower than the rate for mild steel.

Table III. Electrochemical Corrosion of Waste Form and Canister Alloys in J-13 Well Water

Alloy (in wt%)	Corrosion Rates (MPY*) pH=2	pH=4	pH=7	pH=10
SS-15Zr	0.1-0.4	0.08-0.2	0.02-0.08	0.01-0.02
SS-15Zr-2Ru-1.5Pd-0.5Ag	0.4-0.5	0.2	0.04-0.1	0.06-0.09
Zr-8SS	0.02-0.08	0.05-0.06	0.02-0.03	0.01
Zr-8SS-1Ru-1Mo-0.5Pd	0.08	0.04	0.03	0.01
Zirconium	0.02	0.1	0.06-0.09	0.07
Type 304 SS	0.1	0.05	0.05	0.03
Type 316SS	0.3	0.05	0.04	0.03
Incoloy 825	0.03	0.05	0.07	0.03
Cu-7Al (CDA614)	2.3	6.9	3.6	2.0
A106 Grade B low alloy steel	50	23	12	12

*MPY = mils per year. Number ranges indicate multiple measurements.

VI. SUMMARY

The development of the SS-Zr alloy system was pursued under the premise that alloying remnant metallic wastes from the electrometallurgical treatment of spent nuclear fuel will result in waste form alloys with favorable properties for repository disposal. This premise has been shown to be valid, and the SS-15Zr and Zr-8SS alloys were selected as nominal waste form alloys for stainless steel-clad and Zircaloy-clad fuels, respectively.

The alloy microstructures have been characterized to provide baseline data for the evaluation of NMFP and actinide inclusion. The as-cast SS-15Zr alloy has been characterized by using SEM methods to identify phase morphologies and compositions and by using X-ray and neutron diffraction to quantify the crystal structures of the individual phases. Future work on the baseline alloys will include investigations into the microstructural evolution of the Zr_6Fe_{23} phase and the full characterization of the phases in the Zr-8SS waste form.

The NMFPs from spent fuel are present in small quantities and are distributed in solid solution in both phases of the SS-15Zr alloy. A similar distribution is observed in the Zr-8SS alloy, but this system is not yet well characterized. Actinide metals will only be placed in a metal waste form if the ceramic waste form is not used for actinide disposition. Actinides

slightly modify the phase morphology of the alloys, but full characterization data have not been obtained to evaluate changes in the crystal structure. For both NMFP and actinide additions, future work will include the characterization of crystal structure modifications and performance-related effects. Corrosion tests have shown that the metal waste form alloys are highly corrosion resistant, both with and without the presence of NMFPs. A similar set of corrosion tests is being pursued for actinide-bearing alloys.

ACKNOWLEDGMENTS

The authors would like to acknowledge J. K. Basco and P. A. Hansen for their supporting efforts in this work.

REFERENCES

1. S. M. McDeavitt, J. Y. Park, and J. P. Ackerman, "Defining a Metal-Based Waste Form for IFR Pyroprocessing Wastes," *Actinide Processing: Methods and Materials*, eds. B. Mishra and W. A. Averill, pp. 305-319, Minerals, Metals, & Materials Society, Warrendale, Pennsylvania (1994).

2. D. P. Abraham, S. M. McDeavitt, and J. Y. Park, "Microstructure and Phase Identification in Type 304 Stainless Steel-Zirconium Alloys," Accepted for publication in *Metall. and Mater. Trans.* (1996).

3. D. P. Abraham, S. M. McDeavitt, and J. Y. Park, "Metal Waste Forms from the Electrometallurgical Treatment of Spent Nuclear Fuel," *Proc. DOE Spent Nuclear Fuel & Fissile Material Management*, Reno, Nevada, June 16-20, 1996, American Nuclear Society, LaGrange Park, Illinois (1996).

4. D. D. Keiser, Jr. and S. M. McDeavitt, "Actinide-Containing Metal Disposition Alloys," *Proc. DOE Spent Nuclear Fuel & Fissile Material Management*, Reno, Nevada, June 16-20, 1996, American Nuclear Society, LaGrange Park, Illinois (1996).

5. A. J. G. Ellison, J. J. Mazer, and W. L. Ebert, *Effect of Glass Composition on Waste Form Durability: A Critical Review*, Argonne National Laboratory Report ANL-94/28 (1994).

6. *High-Level Waste Borosilicate Glass, A Compendium of Corrosion Characteristics*, ed. J. J. Cunnane, Vol. 1, U.S. Department of Energy Report DOE-EM-0177 (1994).

7. J. E. Battles, J. J. Laidler, C. C. McPheeters, and W. E. Miller, "Pyrometallurgical Process for Recovery of Actinide Elements," *Actinide Processing: Methods and Materials*, eds. B. Mishra and W.A. Averill, pp. 135-151, Minrals, Metals, & Materials Society, Warrendale, Pennsylvania (1994).

8. E. C. Gay and W. E. Miller, "Electrorefining N Reactor Fuel," *Proc. DOE Spent Nuclear Fuel Challenges and Initiatives*, Salt Lake City, Utah, Dec. 13-16, 1994, p. 267, American Nuclear Society, LaGrange Park, Illinois (1994).

9. J. P. Ackerman, "Chemical Basis for Pyrochemical Reprocessing of Nuclear Fuel," *Ind. Eng. Chem. Res.* **30**, 29 (1991).

10. L. C. Walters, B. R. Seidel, and J. H. Kittel, "Metallic Fuels and Blankets in LMFBRs," Nucl. Technol., **65**, 179 (1984).

11. B. R. Westphal, D. D. Keiser, R. H. Rigg, and D. V. Laug, "Production of Metal Waste Forms from Spent Fuel Treatment," *Proc. DOE Spent Nuclear Fuel Challenges and Initiatives*, Salt Lake City, Utah, Dec. 13-16, 1994, p. 288, American Nuclear Society, LaGrange Park, Illinois (1994).

12. Y. Liu, S. M. Allen, and J. D. Livingston, "An Investigation of Fe_3Zr Phase," Scripta Metall. et Mater., **32**, 1129 (1995).